

ONE-SIDED FATTENING OF THE GRAPH IN THE REAL PROJECTIVE PLANE

JAERYOO CHOY AND HAHNG-YUN CHU

Dedicated to the late Professor Bumsig Kim

ABSTRACT. The one-sided fattenings (called semi-ribbon graph in this paper) of the graph embedded in the real projective plane \mathbb{RP}^2 are completely classified up to topological equivalence. A planar graph (i.e., embedded in the plane), admitting the one-sided fattening, is known to be a cactus boundary. For the graphs embedded in \mathbb{RP}^2 admitting the one-sided fattening, unlike the planar graphs, a new building block appears: a bracelet along the Möbius band, which is not a connected summand of the oriented surfaces.

1. Introduction

1.1. General perspective

The idea of fattening or thickening of a graph is not confined in the graph theory but prevails across mathematics and physics, notably the knot theory and its related algebras in the construction of quantum knot invariants. A basic principle is to regard a graph embedded in a higher dimensional manifold as an embedded Riemann surface with boundary via fattening, and then to calculate physics theories defined over the Riemann surface as lit in the quantum field theory predictions ([9] and the references therein). In the broad array, the perspectives entangled with Riemann surfaces have unleashed numerous prospects and problems in contemporary mathematics and physics over decades and furthermore has interacted with higher dimensional geometries via various dualities. With the scope, we have pursued geometric and topological dynamical systems, narrowly a study of flows on Riemann surfaces; particularly in this paper, to reach out a purely graph-theoretic question.

Received December 29, 2020; Accepted September 9, 2021.

2010 *Mathematics Subject Classification.* Primary 05C10, 05C38, 37C10.

Key words and phrases. Fattening, one-sided fattening, graph, ribbon graph, semi-ribbon graph, pre-semi-ribbon graph, Riemann surface, real projective plane, planar graph.

The first author was supported by the National Research Foundation of Korea (NRF) grant funded by the Korea government (MSIT) (No. 2021R1C1C2011737). The second author was supported by research fund of Chungnam National University.

1.2. One-sided fattening and the dynamical systems

The fattening of a planar graph usually stands for the two-sided fattening, frequently alias ribbon graph in the literatures as depicted in the first one in Fig. 1. In contrast, a fattening in this paper means a semi- or hemi-version of the classical one. Thus a one-sided fattening makes sense, which was referred to as a pre-semi-ribbon graph in the precedent work of the authors [3], depicted in the latter two in Fig. 1.

The reader may be aware of that the terminology ‘semi-ribbon’ graph is missing, but we used the term in a rather specific sense in loc. cit.

For a connected graph, a semi-ribbon graph is a one-sided fattened graph whose (1-dimensional) boundary has precisely the two connected components: the whole graph itself and a nearby cycle (called the smooth boundary in our context). As an axiom we presume the nearby cycle as a full Eulerian cycle and thus manifestly illuminates the meaning of one-sided fattening.

The semi-ribbon graph tightly pertains to the dynamo-systematic problem of real analytic flows. Under the assumption that a real analytic flow on \mathbb{R}^2 has a limit set (alias the ω -limit set) being a graph, the trajectory of the flow covers only one side of the graph (as was observed in [5] and [7]). Along the vein, the global attractors of analytic and polynomial flows on \mathbb{R}^2 are characterized up to homeomorphisms in [8].

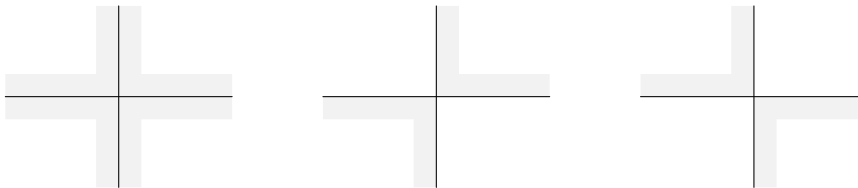


FIGURE 1. Two-sided and one-sided (local) fattenings of a graph

1.3. Main assertion

A graph $\Gamma = (E, V)$ in this paper always means a finite one, i.e., the edge and vertex sets E, V are both finite.

A *cactus* is a union of finitely many (planar) disks which mutually intersect at most one point, and furthermore the union is contracted to a point (Fig. 2 with a semi-ribbon graph, see Definition 2.2 for the semi-ribbon graph).

The real projective plane $\mathbb{R}\mathbb{P}^2$ is the union of the Möbius band M and the disk D^2 identified along their boundary circles. A *bracelet* in M is a chain of embedded circles as in the planar diagram Fig. 3 (see Definition 2.10 for rigor).

A cactal bracelet means a union of a bracelet and finitely many disjoint cactus boundaries in D^2 which intersect the bracelet precisely at a point respectively. See Fig. 4, but a precise definition will be given in §2.4.

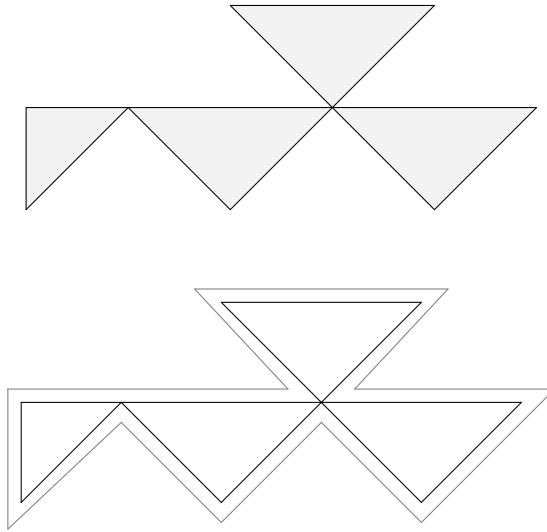


FIGURE 2. A cactus and a semi-ribbon graph (with the fattened area replaced by its boundary in gray)

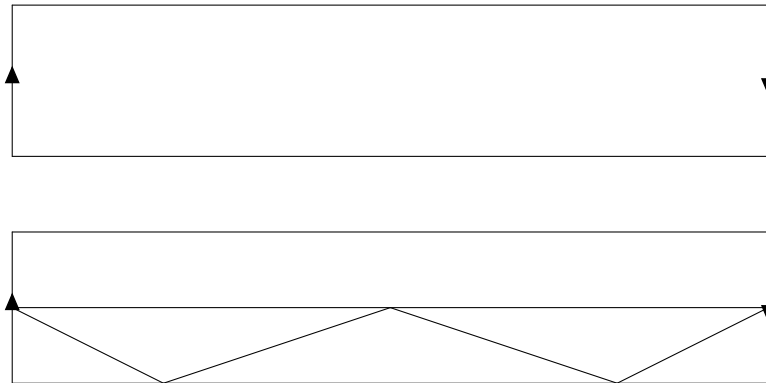


FIGURE 3. The planar diagram of a Möbius band M and a bracelet with two beads in M

The main assertion of this paper is as follows.

Theorem 1.1. *Any semi-ribbon graph in the real projective plane \mathbb{RP}^2 is topologically either the semi-ribbon graph of a cactus boundary as in Fig. 2 or the one of a cactal bracelet as in Fig. 5.*

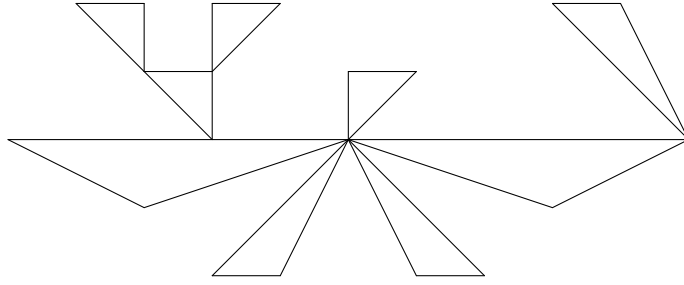


FIGURE 4. A cactal bracelet: a union of a two-bead-bracelet and three cactus boundaries

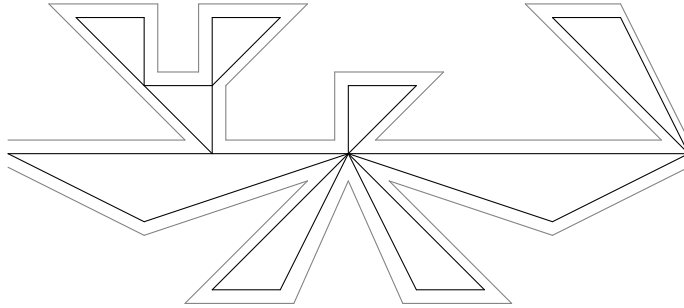


FIGURE 5. A semi-ribbon graph of the cactal bracelet in Fig. 4

1.4. Further motivations

In the precedent co-works, we studied surface flows (e.g. [3]) and space flows ([4]) in the view of dynamical systems. Aforementioned in §1.1 partly, surface flow and the underlying embedded graph theory have been studied as a part of the 2d quantum field theory and the 2d gauge theory. This direction has been kept coherent in the first named author's works (see e.g. [2, Appendix B] and the references therein) with a symmetry between 2d-4d (e.g. [6, 11]).

What we know or allege is the characterization of the semi-ribbon graphs embedded in the oriented surfaces [3]: it was asserted that the semi-ribbon graphs are only the cactus boundaries. Therefore these graphs are far narrowly categorized in the even-valent graphs (amounting to the ones with a full Eulerian cycle). See a quick example of an even-valent planar graph Fig. 6 which admits a semi-ribbon graph in \mathbb{RP}^2 but never in any oriented surfaces.

Let us start from any even-valent graph Γ , which is embedded in the space \mathbb{R}^3 without loss of generality. Let us fatten Γ in two sides in the classical sense

of the first figure in Fig. 1, so that Γ lies in the interior of the fattened band. A well-known question is cast as:

capping off all the boundary circles with disks respectively,
what (oriented or unoriented) surface do we get?

The embedding of the given graph into the resulting surface is called *map* ([9, Definition 1.3.6]), which we do *not* use the terminology any longer in this paper to be safe from the confusing dilogy. As there are plural but finite ways of two-sided fattenings in \mathbb{R}^3 up to isotopy, we have crumbles for the above question, e.g. the genus problem of the given graph ([10, §4.5]) and knot invariants ([9, §6.2]).

In this paper, we adapted the ad hoc assumption that there exists a capping disk whose boundary becomes a full Eulerian cycle of the given graph. Note that any knot in \mathbb{R}^3 is realized in this way (without the assumption, one has a link in general). On the other hand, the two-bead-bracelet Fig. 6 epitomizes a sharp contrast in the genera of the resulting surfaces vis-a-vis the orientations in the above question. It admits a semi-ribbon graph (cf. Fig. 5), however

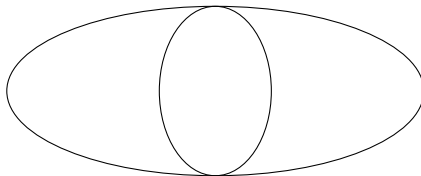


FIGURE 6.

never as a graph embedded in any oriented surface because it is not a cactus boundary as asserted in [3].

With the above question in mind, we study of the elemental building block \mathbb{RP}^2 of the resulting closed unoriented surface. We hope to structure the semi-ribbon graphs embedded in closed unoriented surfaces (cf. [10, §4.4]). Manifestly we do not expect a succinct answer with a full description, since any even-valent graphs other than the cactus boundaries, e.g. the complete graphs K_{2n+1} , $n \geq 2$, are all included in this category. To see a complexity of the resulting surfaces, let us add two more non-loop edges to Fig. 6. Then the resulting surface is the Klein bottle.

We wrap up the introduction with coloration of the surface containing the semi-ribbon graph, onto which was drawn our attention by an anonymous referee. So far the surfaces which are either an oriented surface or \mathbb{RP}^2 , are always 2-colorable.

The contents of paper. Section 2 settles the prerequisites of one-sided fattening, called semi-ribbon graph. It also recaps a semi-ribbon graph emerging from ‘oriented’ graph to invoke an origin of our problem sitting in the dynamical

systems. A multi-layer structure of a graph embedded in a surface is introduced in this section. With these preliminaries, we prove the main theorem in Section 3 of the topological classification of the semi-ribbon graphs in \mathbb{RP}^2 . Appendix recaps the topological classification of the planar semi-ribbon graphs, as an application of the multi-layer structure.

Acknowledgement. J. Choy is grateful to Professor Bumsig Kim for his support to J. Choy's series lectures on D-modules on Riemann surfaces and for the hospitality of research environments.

2. Preliminary: pre-semi-ribbon graph, semi-ribbon graph, multi-layers and cactal bracelet

For a given graph embedded in a surface, we give the definitions of pre-semi-ribbon graph and semi-ribbon graph in §2.1 and then the multi-layered structure in §2.3. A cactal bracelet is also studied in §2.4 as a new class in the case \mathbb{RP}^2 . By these three subsections we are ready for the proof of Main theorem. In §2.2, we explain the origin of the semi-ribbon graphs from the dynamical systems.

By a graph $\Gamma = (E, V)$, we consistently mean a finite graph which consists of finite sets E, V of edges and vertices respectively. A graph is called *even-valent* if every vertex has even valency, i.e., the even number of adjoining edges (a loop is counted twice).

2.1. Pre-semi-ribbon graph and semi-ribbon graph

Definition 2.1. Let $\Gamma = (E, V)$ be a connected even-valent graph embedded in the interior of a 2-dimensional topological manifold S with the non-triviality assumption $E \neq \emptyset$. A *pre-semi-ribbon graph* of Γ , denoted Γ_{psr} , is a compact subset of S such that for every point of Γ there exists an open neighborhood whose intersection with Γ_{psr} is alternating.

See Fig. 7 for the alternating fattening at a vertex of valency 4, where the gray area and the black line segments denote Γ_{psr} and Γ , respectively. In the below hereafter, the gray areas are replaced by the boundary components other than Γ , so called the smooth boundary. See also Item (7) below.

Let us draw quick anecdotes from the above definition, plus convention for the later part and the more induced definitions.

- (1) Since every point of Γ assumes of even valency, the 'alternating' makes sense.
- (2) The one-sided fattening also makes sense due to the alternating axiom. As aforementioned in Introduction, the two-sided fattening is classically known as a ribbon graph, which legitimates the notions, pre-semi-ribbon graph, or semi-ribbon graph below.
- (3) In our figures from now on, rather than shading the full fattened area, we plot its boundary, which suffices and would be even succincer in our purpose.

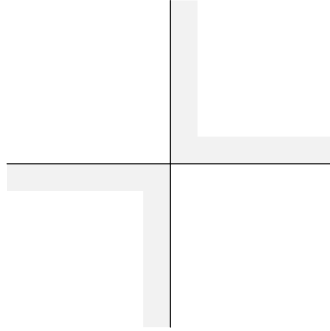


FIGURE 7. Local depiction of pre-semi-ribbon graph at a vertex of valency 4

- (4) The boundary $\text{Bd}(\Gamma_{\text{psr}})$ is a disjoint union of Γ and (topologically embedded) circles such that locally these circles are locally sitting in alternating sectors of Γ . This property can be an alternative to define Γ_{psr} . Ref. Item (8) below.
- (5) Near at a non-vertex of Γ , $\text{Bd}(\Gamma_{\text{psr}})$ is homeomorphic to the union of (local) Γ and its parallel shift, as depicted in Fig. 8.



FIGURE 8. Local depiction of the boundary $\text{Bd}(\Gamma_{\text{psr}})$ of a pre-semi-ribbon graph Γ_{psr} at a non-vertex point or a bivalent vertex of Γ

- (6) Near at a vertex of Γ , $\text{Bd}(\Gamma_{\text{psr}})$ is homeomorphic to the union of (local) Γ and its alternating nearby hyperbolas, as depicted in Fig. 9.
- (7) In both of the above figures, the black line segments are parts of the given graph Γ while gray ones are new boundary of the fattening Γ_{psr} . Therefore

$$\text{Bd}(\Gamma_{\text{psr}}) = \Gamma \sqcup \text{Bd}_{\text{sm}}(\Gamma_{\text{psr}}) \quad (\text{disjoint union})$$

where the latter component represents the gray segment. The notation $\text{Bd}_{\text{sm}}(\Gamma_{\text{psr}})$ stands for the *smooth* boundary, as an obvious small deformation of Γ_{psr} renders the new boundary smooth (in our topological context, the smoothness is never essential, but just for expediency).

- (8) Now one can see immediately that even without the assumption that $\text{Bd}_{\text{sm}}(\Gamma_{\text{psr}})$ is a disjoint union of circles, it must be from the above observation of local smooth boundary. Indeed, as $\text{Bd}_{\text{sm}}(\Gamma_{\text{psr}})$ is locally homeomorphic to an open interval, now the compactness of Γ deduces that $\text{Bd}_{\text{sm}}(\Gamma_{\text{psr}})$ is a disjoint union of finitely many circles.

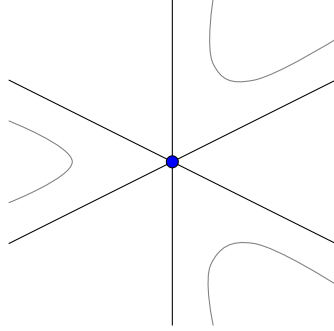


FIGURE 9. Local depiction of the boundary $\text{Bd}(\Gamma_{\text{psr}})$ of a pre-semi-ribbon graph Γ_{psr} at a vertex with valency 6

Definition 2.2. With the ad hoc assumption that $\text{Bd}_{\text{sm}}(\Gamma_{\text{psr}})$ is connected, i.e., an embedded circle, we say Γ_{psr} *semi-ribbon graph* of Γ , denoted Γ_{sr} .

2.2. Remarks on pre-semi-ribbon graph of an oriented graph

This subsection is intended to introduce pre-semi-ribbon graph of an oriented graph previously studied in [3]. Let us briefly explain where the orientation comes from. First a given real analytic flow on \mathbb{R}^2 is assumed to have the singular locus as isolated points and to have its ω -limit set as a graph. Hence the orientation of the ω -limit graph is inherited from the flow. The vertices of valency ≥ 3 of the limit graph are singular points of the flow. Combined with the well-known theorem of Bendixon [1], each sector with a vertex center is necessarily hyperbolic (Fig. 10).

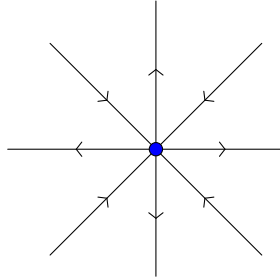


FIGURE 10. Hyperbolic vertex

As a result each sector (whose center is not necessarily a vertex but any point of the graph) attains an orientation, which is called an oriented sector. Now a pre-semi-ribbon graph is defined for an oriented sector.

Definition 2.3 ([3, Definitions 3.2, 3.3]). Let Γ be an oriented planar graph. A compact subset of \mathbb{R}^2 is a *pre-semi-ribbon graph* Γ_{psr} of Γ if there is a set of open neighborhoods U_x of $x \in \Gamma$ in \mathbb{R}^2 covering Γ_{psr} such that for each oriented sector T centered at x , there exists an orientation-preserving homeomorphism $\phi_x: (U_x, T) \cong (B_0, B_0^{\geq 0})$ satisfying

$$(1) \quad \phi_x(\Gamma_{\text{psr}} \cap T) = B_0^{[0,1/2]}, \quad \phi_x(\text{Bd}(\Gamma_{\text{psr}}) \cap T) = B_0^0 \sqcup B_0^{1/2}$$

and for each non-oriented sector T , $\Gamma_{\text{psr}} \cap \text{Int}(T) = \emptyset$. Here the notation and the orientation convention are subject to the following. B_0 is the radius 1 closed ball in \mathbb{R}^2 centered at the origin and B_0^I denotes the subset of B_0 with constraint of the vertical coordinate $y \in I$, e.g., $B_0^{\geq 0}$ is the upper hemi-disc. The orientation of \mathbb{R}^2 obeys the counter-clock direction and its subsets, except T , have inherited ones. And a sector T in U_x is oriented if the two separatrices are distinct and the arrows associated to them are heading from left to right via ϕ_x . See Fig. 11.

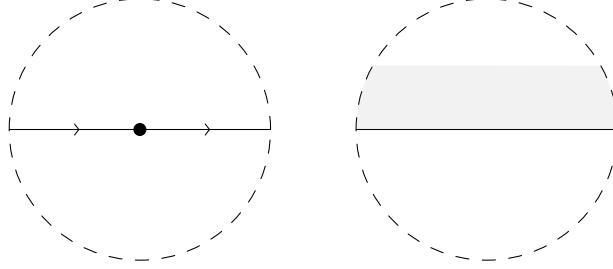


FIGURE 11. An oriented sector and the (local) pre-semi-ribbon graph

2.3. Multi-layer structure

A graph embedded in any surface (with an infinity fixed) admits a layered structure by peeling off from the infinity. This subsection mostly concentrates on properties of the layer structure of the planar graphs, as our primary concern is $\mathbb{R}\mathbb{P}^2$ whose 2-fold cover is the 2-sphere S^2 . In Appendix we will illustrate its application to the planer semi-ribbon graphs as a mild introduction. Hence the reader looking for a warm-up before the proof of Main theorem in §3, can read Appendix first.

Definition 2.4. Let us declare any point of a closed surface S the infinity ∞ . For a graph Γ embedded in $S \setminus \infty$, the *shell* subgraph $\Gamma^S = (E^S, V^S)$ is the subgraph of Γ whose points can be path-connected to the infinity ∞ in the complement $S \setminus \Gamma$.

The *kernel* subgraph $\Gamma^K = (E^K, V^K)$ is the subgraph of Γ defined by setting

$$E^K := E \setminus E^S, \quad V^K := V \setminus V^S \cup \text{the set of endpoints of edges in } E^K.$$

Note in the above definition that the layers are finitely many, equally, peeling off the out layers is an exhaustive procedure. See an example of a multi-layered planar graph in Fig. 12.

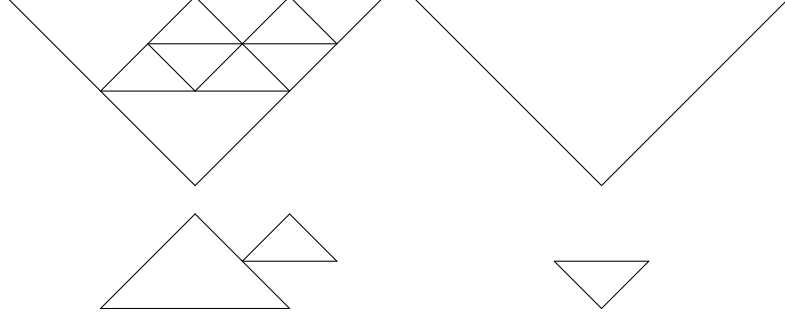


FIGURE 12. The multi-layers of the planar graph in the upper left corner: upper right one is the first layer, lower left one is the second and the lower right one is the third.

Definition 2.5. Suppose the surface $S = S^2$ and a graph Γ is embedded in S^2 . By choosing ∞ outside Γ , we have $\Gamma \subset \mathbb{R}^2 = S \setminus \infty$, i.e., a planar graph. For a planar graph Γ , we define the *hull* $\widehat{\Gamma}$ as the (compact) subset of \mathbb{R}^2 with all the simple cycles of Γ filled into the disks. Here, ‘simple’ means no self-intersection point. By the construction, $\widehat{\Gamma}$ is simply connected, hence contractible to a point.

Definition 2.6. A *tree* Γ means a planar graph such that $\Gamma = \widehat{\Gamma}$, i.e., no cycle allowed, hence contractible to a point. Each edge of a tree is called a *stem* in this paper.

We say a planar graph Γ a *cactal tree* if $\Gamma = \widehat{\Gamma} \setminus \text{Int}(\widehat{\Gamma})$ where Int stands for the interior in \mathbb{R}^2 . Obviously, any planar tree and any cactus boundary are cactal trees. Observe that a cactal tree consists of the stems and the cactal blades, depending on if the interiors are empty or not. See Fig. 13.

We say an edge of a planar graph Γ is an *internal edge* if it is contained in the interior $\text{Int}(\widehat{\Gamma})$.

Lemma 2.7. Let $\Gamma = (E, V)$ be a connected planar graph with $E \neq \emptyset$. Then $\Gamma = \Gamma^{\text{S}}$, equivalently Γ has the empty kernel subgraph, if and only if Γ is a cactal tree.

Proof. This assertion is obvious since every internal edge lies in the kernel Γ^{K} . \square

Lemma 2.8. Let $\Gamma = (E, V)$ be a connected planar graph with $E \neq \emptyset$. If Γ is even-valent, then the shell subgraph Γ^{S} is a cactus boundary. Hence the kernel subgraph Γ^{K} is even-valent.

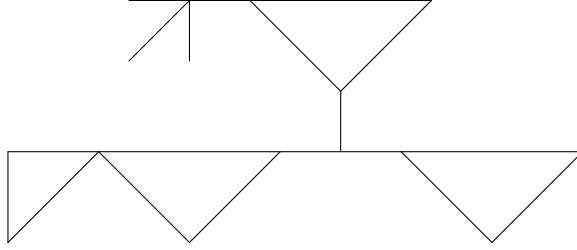


FIGURE 13. A cactal tree

Proof. If there would be a stem in the shell cactal tree Γ^S (Lemma 2.7), then there does not exist a full Eulerian cycle since a stem is one-way. Since the kernel Γ^K is contained in the hulls of cactal blades of Γ^S , Γ neither allows a full Eulerian cycle. However this is absurd to the fact that the even-valency amounts to the existence of a full Eulerian cycle.

The second assertion is obvious from that a cactus boundary, e.g. Γ^S , is even-valent. Indeed at every vertex there are even numbers of the adjoining edges from Γ^S , hence from Γ^K by counting the leftover edges. \square

Lemma 2.9. *Suppose that a connected planar graph Γ with $E \neq \emptyset$ admits a semi-ribbon graph Γ_{sr} and furthermore that the smooth boundary $\text{Bd}_{\text{sm}}(\Gamma_{\text{sr}})$ is path-connected to the infinity in $\mathbb{R}^2 \setminus \Gamma$. Then Γ is a cactus boundary with the outward Γ_{sr} as in Fig. 2.*

Proof. The assumption of the path-connectedness implies that $\text{Bd}_{\text{sm}}(\Gamma_{\text{sr}})$ is not arbitrarily close to the kernel Γ^K , which means $\Gamma = \Gamma^S$. Now by Lemma 2.8, Γ is a cactus boundary and the semi-ribbon graph is necessarily as in Fig. 2. \square

2.4. Cactal bracelet

Identifying $\mathbb{RP}^2 = S^2/(\mathbb{Z}/2\mathbb{Z})$ where the group $\mathbb{Z}/2\mathbb{Z}$ acts antipodal, let $p: S^2 \rightarrow \mathbb{RP}^2$ be the natural projection. For a given graph Γ or its semi-ribbon graph Γ_{sr} in \mathbb{RP}^2 , we declare the north pole of S^2 denoted ∞ , which always assumes to avoid $p^{-1}(\Gamma), p^{-1}(\Gamma_{\text{sr}})$. Let D, D' be the upper and lower hemispheres of S^2 , respectively. Frequently we identify $S^2 \setminus \infty \cong \mathbb{R}^2$ via the stereographic projection, so that the restriction $p: \mathbb{R}^2 \rightarrow \mathbb{RP}^2$ makes sense. We also keep the same notation p as various restriction maps of the original one.

Definition 2.10. A graph Γ in \mathbb{RP}^2 is a *cactal bracelet* if its pullback $p^{-1}(\Gamma)$ in $D \setminus \infty \subset \mathbb{R}^2$ is a union of the pullback B of a bracelet and finitely many cactus boundaries E_1, E_2, \dots such that the hull \widehat{B} (as a planar graph) and each \widehat{E}_i intersect precisely at one point, and \widehat{E}_i are mutually disjoint.

For examples of cactal bracelets, see Fig. 3 and Fig. 4.

3. Proof of Main theorem

In this section we prove Main Theorem 1.1, which we proceed in §3.2 after listing in §3.1 the notations upon the needs for the proof.

3.1. Notations

The north pole $\infty \in D \subset S^2 = D \cup D'$ maps via the projection $p: S^2 \rightarrow \mathbb{RP}^2$ to a point in $\mathbb{RP}^2 \setminus \Gamma_{\text{sr}}$, again denoted ∞ . We may assume that ∞ is path-connected to the smooth boundary $\text{Bd}_{\text{sm}}(\Gamma_{\text{sr}})$ in $\mathbb{RP}^2 \setminus \Gamma$.

Recall that $D \setminus \infty$ is identified with $\mathbb{R}^2 \setminus \text{Int}(D')$ via the stereographic projection, where Int denotes the interior. Recall also that by the same notation p , we denote various restrictions $p|_D, p|_{D \setminus \infty}, p|_{\text{Int}(D)}, p|_{\text{Bd}(D)}$ to \mathbb{RP}^2 . Note that $p: S^2 \rightarrow \mathbb{RP}^2$ and the restriction to $\text{Int}(D)$ is a homeomorphism while the restriction to $\text{Bd}(D)$ mapping onto the meridian C of \mathbb{RP}^2 is of $2:1$.

The equator $\text{Bd}(D)$ is the union of two semicircles, denoted C_1, C_2 , such that the restrictions $p: C_i \rightarrow C$ are homeomorphisms except the two endpoints mapping to a point.

Let $\tilde{\Gamma} := p^{-1}(\Gamma)$ in D . If $C \subset \Gamma$, then C_1, C_2 are subgraphs of $\tilde{\Gamma}$.

3.2. Proof of Theorem 1.1

Now the proof goes in the two cases depending on if there is a cycle of Γ non-contractible to a point in \mathbb{RP}^2 . If all the cycles of Γ are contractible, using a homeomorphism of \mathbb{RP}^2 , we may assume that all $\Gamma, \text{Bd}_{\text{sm}}(\Gamma_{\text{sr}})$ and ∞ lie in the open disk $p(\text{Int}(D))$ of \mathbb{RP}^2 , and moreover that ∞ is path-connected to $\text{Bd}_{\text{sm}}(\Gamma_{\text{sr}})$ in $p(D \setminus \Gamma)$. Indeed what we need to prove is that Γ is contractible to a point in \mathbb{RP}^2 . Since any simple cycle of Γ is the boundary of a disk embedded in \mathbb{RP}^2 , shrinking the disks one-by-one enables Γ to have no cycles in the first place, hence a tree. Likewise, shrinking the edges of the tree assures the contractibility of Γ to a point in \mathbb{RP}^2 .

Pulled back along the homeomorphism $p: \text{Int}(D) \rightarrow p(\text{Int}(D))$, $p^{-1}(\Gamma_{\text{sr}})$ is a semi-ribbon graph of $\tilde{\Gamma} = p^{-1}(\Gamma)$. Thus by Lemma 2.9, $p^{-1}(\Gamma_{\text{sr}})$ is the outward semi-ribbon graph of a cactus boundary and $\tilde{\Gamma}$ is the cactus boundary as in Fig. 2. This completes the proof of the first case.

What is left is the case when there is a cycle non-contractible to a point. We may assume the cycle is a simple one, so that it can be set the median C , because the fundamental group $\pi_1(\mathbb{RP}^2) \cong \mathbb{Z}/2\mathbb{Z}$ is generated by C .

We claim that only one of C_1, C_2 is arbitrarily close to $p^{-1}(\text{Bd}_{\text{sm}}(\Gamma_{\text{sr}})) \cong S^1$. Since $C \subset \Gamma$ is arbitrarily close to $p^{-1}(\text{Bd}_{\text{sm}}(\Gamma_{\text{sr}}))$, so is at least one of C_1, C_2 , say C_1 , to $p^{-1}(\text{Bd}_{\text{sm}}(\Gamma_{\text{sr}}))$. We are left to prove that C_2 is not arbitrarily close to $p^{-1}(\text{Bd}_{\text{sm}}(\Gamma_{\text{sr}}))$. If C_2 also would be arbitrarily close to $p^{-1}(\text{Bd}_{\text{sm}}(\Gamma_{\text{sr}}))$, then $p^{-1}(\text{Bd}_{\text{sm}}(\Gamma_{\text{sr}}))$ is arbitrarily close to both C_1, C_2 and thus Γ_{sr} fattens C two-sided in \mathbb{RP}^2 . This violates the one-sidedness of semi-ribbon graphs.

Let Γ' be the subgraph of $\tilde{\Gamma}$ in \mathbb{R}^2 which is arbitrarily close to the circle $p^{-1}(\text{Bd}_{\text{sm}}(\Gamma_{\text{sr}}))$. Since by the above claim, C_1 is arbitrarily close to $p^{-1}(\text{Bd}_{\text{sm}}(\Gamma_{\text{sr}}))$ while C_2 is not, Γ' is the closure of $\tilde{\Gamma} \setminus C_2$ in \mathbb{R}^2 .

With $\tilde{\Gamma}, \Gamma', \text{Bd}_{\text{sm}}(\Gamma_{\text{sr}}), D'$ embedded in \mathbb{R}^2 via p^{-1} , we claim the following:

- (1) Γ' admits a semi-ribbon graph in \mathbb{R}^2 with the smooth boundary $\text{Bd}_{\text{sm}}(\Gamma'_{\text{sr}}) = p^{-1}(\text{Bd}_{\text{sm}}(\Gamma_{\text{sr}}))$. Equivalently Γ' is a cactus boundary, or the hull $\hat{\Gamma}'$ is a cactus.
- (2) The hull $\hat{\Gamma}'$ contains the disk D' .

We complete the proof admitting the claims for a while. Since the hull $\hat{\Gamma}'$ is a cactus containing the disk D' , there is a disk component of the cactus $\hat{\Gamma}'$ containing D' , which is denoted D'' . We know that C_1 is a subset of $\Gamma' = \text{Bd}(\hat{\Gamma}')$, hence of $\text{Bd}(D'')$. We can write the circle boundary

$$\text{Bd}(D'') = C_1 \cup C'_2,$$

where C'_2 is a simple subpath of Γ' whose terminal vertices coincide with the ones of C_1 respectively. It is immediate that C_1 and C'_2 together are projected via p to the bracelet of the Möbius strip of \mathbb{RP}^2 as in Fig. 3 (recall C_1 projects to the median). Hence summing up our argument, we obtain the description of the semi-ribbon graph of a cactal bracelet as in Fig. 5.

It remains to check the claim. We prove Item (2) first. This amounts to that the circle $p^{-1}(\text{Bd}_{\text{sm}}(\Gamma_{\text{sr}}))$ encloses D' . We observe that the circle $p^{-1}(\text{Bd}_{\text{sm}}(\Gamma_{\text{sr}}))$ dissects \mathbb{R}^2 into two connected components, and recall that $p^{-1}(\Gamma)$ is contained in the bounded component. As $C_1 \subset p^{-1}(\Gamma) \cap D'$, it is also contained in the bounded component. So is D' , which proves Item (2).

For Item (1), the premise that Γ' is arbitrarily close to $p^{-1}(\text{Bd}_{\text{sm}}(\Gamma_{\text{sr}}))$, assures that it is path-connected to ∞ . Therefore Γ' equals its shell $(\Gamma')^{\text{S}}$. By Lemma 2.7, it is a cactal tree. We prove there is no stem in the cactal tree Γ' . By Item (2), any stem intersects $\mathbb{R}^2 \setminus D'$. However no edge of Γ' lying outside D' is two-sided fattened by $p^{-1}(\Gamma_{\text{sr}})$. This forces no stem in Γ' . \square

Appendix A. Pre-semi-ribbon and semi-ribbon graphs of the planar graphs

In the appendix we illustrate an application of the multi-layer structure to the planar graphs. This structure can be put differently in terms of the 2-coloration as the even-valent planar graphs are 2-colorable, aforementioned in §1.4.

A.1. Pre-semi-ribbon graphs of the planar graphs

Proposition A.1. *Whenever Γ is a connected even-valent planar graph with $E \neq \emptyset$, it admits a pre-semi-ribbon graph Γ_{psr} . Moreover there are precisely two pre-semi-ribbon graphs up to deformation: inward and outward.*

Proof. We apply the induction hypothesis on the number of edges thanks to Lemma 2.8. The initial hypothesis is the case $\Gamma = \Gamma^S$, i.e., a cactus boundary by Lemma 2.8. In this case, it is rather easy to see the two pre-semi-ribbon graphs (recall Fig. 2). First observe that a circle allows two pre-semi-ribbon graphs in and outwards. Since a cactus boundary is a connected union of circles, one circle's pre-semi-ribbon graph completely determines all the others' one.

Unless the kernel $\Gamma^K = \emptyset$, both Γ^S, Γ^K admit pre-semi-ribbon graphs only in two ways respectively: in and outwards. If the shell Γ^S has the inward one, then the outward one does Γ^K , because Γ^S, Γ^K have an intersection vertex where the pre-semi-ribbon graphs $\Gamma_{\text{psr}}^S, \Gamma_{\text{psr}}^K$ are merged by rendering them. This rendering is a local problem which enables the alternating fattening in the definition of pre-semi-ribbon graph (Fig. 14). See also Fig. 15 for a (global)

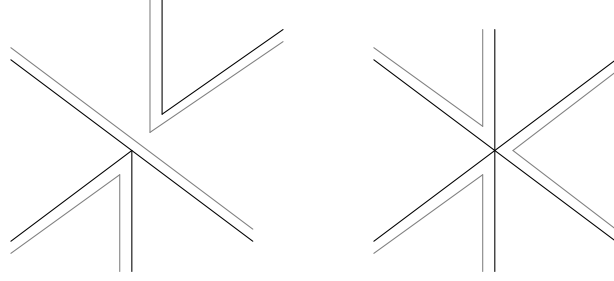


FIGURE 14. A local merging of $\Gamma_{\text{psr}}^S, \Gamma_{\text{psr}}^K$ at an intersection vertex

example. The case of out-in (opposite to the above in-out choice) is similar but easier since $\Gamma_{\text{psr}}^S, \Gamma_{\text{psr}}^K$ are disjoint. The remaining combinations in-in and out-out are impossible to stand by the alternating reason. This completes the proof. \square

A.2. Semi-ribbon graphs of the planar graphs

The semi-ribbon graphs are also reconstructed from the multi-layered structure. Recall that a circle allows the semi-ribbon graphs in the two ways: in and outward, which is the only exception as we will see in the following proposition (cf. [3, Lemma 3.11]).

Proposition A.2. *If a connected planar graph Γ with $E \neq \emptyset$ admits a semi-ribbon graph, then it is either*

- (i) *a cactus boundary or*
- (ii) *the union of cactus boundaries and a circle such that the circle encloses all the cactus boundaries, intersects each cactus boundary precisely at one vertex and the cactus boundaries are mutually disjoint (Fig. 16).*

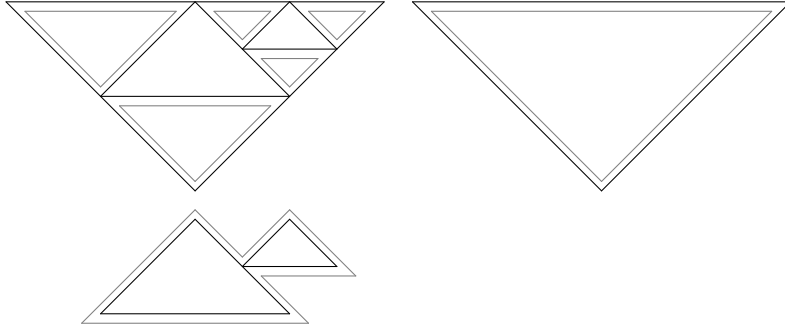


FIGURE 15. Merging pre-semi-ribbon graphs of two layers

Moreover unless Γ is a circle, its semi-ribbon graph Γ_{sr} is given outward, which is unique up to deformation.

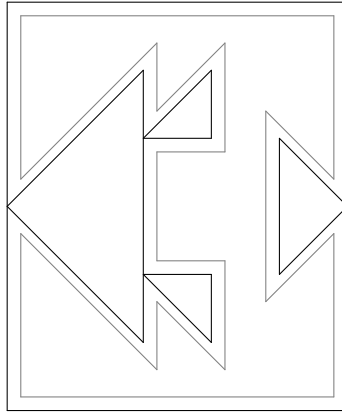


FIGURE 16. The case (ii): a circle encloses mutually disjoint cactus boundaries and intersects each of them once.

Proof. There are several proofs, among which we rely on the multi-layers approach.

Suppose $\Gamma = \Gamma^{\text{S}}$ first. Since Γ is even-valent (by the existence of a semi-ribbon graph), Lemma 2.8 assures the case (i).

Suppose now $\Gamma \neq \Gamma^{\text{S}}$, i.e., $\Gamma^{\text{K}} \neq \emptyset$. Since Γ_{sr} would be a special case of Γ_{psr} , the proof of Proposition A.1 tells that Γ_{sr} is obtained from the rendering of the inward $\Gamma_{\text{psr}}^{\text{S}}$ and outward $\Gamma_{\text{psr}}^{\text{K}}$ because Γ_{sr} should be connected. Furthermore the connectivity of Γ_{sr} implies that Γ^{S} is a circle with the inward $\Gamma_{\text{psr}}^{\text{S}}$.

The connectivity of Γ implies that Γ^S and any connected component (being necessarily a cactus boundary) of Γ^K intersect precisely at one vertex, since otherwise Γ^S would be disconnected through the rendering. See Fig. 16. Hence we get the case (ii).

Note finally that the kernel Γ^{KK} of Γ^K is empty. For, otherwise, Γ_{psr}^{KK} is inward (recall Γ_{psr}^K is outward), which is absurd to the connectivity of Γ_{sr} . As there is no deeper layer, the assertion is proven. \square

Remark A.3. One can unify the above cases (i), (ii) as follows. We compactify the ambient plane \mathbb{R}^2 to the 2-sphere S^2 . Then Γ is again a cactus boundary in S^2 , and Γ_{sr} can be understood outward.

References

- [1] I. Bendixson, *Sur les courbes définies par des équations différentielles*, Acta Math. **24** (1901), no. 1, 1–88. <https://doi.org/10.1007/BF02403068>
- [2] J. Choy, *Geometry of Uhlenbeck partial compactification of orthogonal instanton spaces and the K-theoretic Nekrasov partition functions*, Adv. Math. **330** (2018), 763–809. <https://doi.org/10.1016/j.aim.2018.03.037>
- [3] J. Choy and H.-Y. Chu, *Polycycle omega-limit sets of flows on the compact Riemann surfaces and Eulerian path*, arXiv:1609.08505.
- [4] J. Choy and H.-Y. Chu, *Dynamics of Riemannian 1-foliations on 3-manifolds*, Taiwanese J. Math. **23** (2019), no. 1, 145–157. <https://doi.org/10.11650/tjm/180605>
- [5] J. G. Espín Buendía and V. Jiménez López, *Some remarks on the ω -limit sets for plane, sphere and projective plane analytic flows*, Qual. Theory Dyn. Syst. **16** (2017), no. 2, 293–298. <https://doi.org/10.1007/s12346-016-0192-1>
- [6] K. Intriligator and N. Seiberg, *Mirror symmetry in three-dimensional gauge theories*, Phys. Lett. B **387** (1996), no. 3, 513–519. [https://doi.org/10.1016/0370-2693\(96\)01088-X](https://doi.org/10.1016/0370-2693(96)01088-X)
- [7] V. Jiménez López and J. Llibre, *A topological characterization of the ω -limit sets for analytic flows on the plane, the sphere and the projective plane*, Adv. Math. **216** (2007), no. 2, 677–710. <https://doi.org/10.1016/j.aim.2007.06.007>
- [8] V. Jiménez López and D. Peralta-Salas, *Global attractors of analytic plane flows*, Ergodic Theory Dynam. Systems **29** (2009), no. 3, 967–981. <https://doi.org/10.1017/S0143385708000552>
- [9] S. K. Lando and A. K. Zvonkin, *Graphs on surfaces and their applications*, Encyclopaedia of Mathematical Sciences, 141, Springer-Verlag, Berlin, 2004. <https://doi.org/10.1007/978-3-540-38361-1>
- [10] B. Mohar and C. Thomassen, *Graphs on surfaces*, Johns Hopkins Studies in the Mathematical Sciences, Johns Hopkins University Press, Baltimore, MD, 2001.
- [11] A. Okounkov, *Lectures on K-theoretic computations in enumerative geometry*, in Geometry of moduli spaces and representation theory, 251–380, IAS/Park City Math. Ser., 24, Amer. Math. Soc., Providence, RI, 2017. <https://doi.org/10.1090/pcms/024>

JAERYOO CHOY
 DEPARTMENT OF MATHEMATICS
 CHUNGNAM NATIONAL UNIVERSITY
 DAEJEON 34134, KOREA
Email address: jaeyoochoy@gmail.com, choy@kias.re.kr

HAHNG-YUN CHU
DEPARTMENT OF MATHEMATICS
CHUNGNAM NATIONAL UNIVERSITY
DAEJEON 34134, KOREA
Email address: `hychu@cnu.ac.kr`